Relativistic Coulomb excitation of 88Kr

Moschner, K.; Blazhev, A.; Jolie, J.; Warr, N.; Boutachkov, P.; Bednarczyk, P.; Sieja, K.; Algora, A.; Ameil, F.; Bentley, M. A.; Brambilla, S.; Braun, N.; Camera, F.; Cederkäll, J.; Corsi, A.; Danchev, M.; Dijulio, D.; Fahlander, C.; Gerl, J.; Giaz, A.; Golubev, P.; Górska, M.; Grebosz, J.; Habermann, T.; Hackstein, M.; Hoischen, R.; Kojouharov, I.; Kurz, N.; Mărginean, N.; Merchán, E.; Möller, T.; Naqvi, F.; Nara Singh, B. S.; Nociforo, C.; Pietralla, N.; Pietri, S.; Podolyák, Zs; Prochazka, A.; Reese, M.; Reiter, P.; Rudigier, M.; Rudolph, D.; Sava, T.; Schaffner, H.; Scruton, L.; Taprogge, J.; Thomas, T.; Weick, H.; Wendt, A.; Wieland, O.

Published in:
Physical Review C - Nuclear Physics

DOI:
10.1103/PhysRevC.94.054323

2016

Relativistic Coulomb excitation of ^{88}Kr

K. Moschner,[1] A. Blazhev,[1] J. Jolie,[1] N. Warr,[1] P. Boutachkov,[2,3] P. Bednarczyk,[4] K. Sieja,[5] A. Algora,[6] F. Ameil,[2] M. A. Bentley,[7] S. Brambilla,[8] N. Braun,[1] F. Camera,[8] J. Cederkäll,[9] A. Corsi,[8] M. Danchev,[10] D. DiJulio,[9] C. Fahlander,[9] J. Gerl,[2] A. Giaz,[8] P. Golubev,[9] M. Górska,[2] J. Grebosz,[4] T. Habermann,[2] M. Hackstein,[1] R. Hoischen,[2,9] I. Kojouharov,[2] N. Kurz,[2] N. Mărginean,[11] E. Merchán,[2] T. Möller,[3] F. Naqvi,[1,2] B. S. Nara Singh,[7] C. Nociforo,[2] N. Pietralla,[3] S. Pietri,[2] Zs. Podolyák,[12] A. Prochazka,[2] M. Reese,[3] P. Reiter,[1] M. Rudigier,[1,12] D. Rudolph,[9] T. Sava,[11] H. Schaffner,[2] L. Scruton,[7] J. Taprogge,[1] T. Thomas,[1] H. Weick,[2] A. Wendt,[1] O. Wieland,[8] and H.-J. Wollersheim[2]

[1]*Institut für Kernphysik, Universität zu Köln, Köln, Germany*
[2]*GSI Helmholtzzentrum für Schwerionenforschung GmbH, Darmstadt, Germany*
[3]*Institut für Kernphysik, Technische Universität Darmstadt, Darmstadt, Germany*
[4]*Institute of Nuclear Physics PAN, Kraków, Poland*
[5]*Université de Strasbourg, IPHC, CNRS, UMR7178, Strasbourg, France*
[6]*Instituto de Fisica Corpuscular, CSIC-Universidad de Valencia, Valencia, Spain*
[7]*Department of Physics, University of York, York, United Kingdom*
[8]*Dipartimento di Fisica, Università de Milano, and INFN Sezione Milano, Milano, Italy*
[9]*Department of Physics, Lund University, Lund, Sweden*
[10]*Faculty of Physics, University of Sofia, Sofia, Bulgaria*
[11]*Horia Hulubei NIPNE, Bucharest, Romania*
[12]*Department of Physics, University of Surrey, Guildford, United Kingdom*

(Received 10 February 2015; revised manuscript received 15 February 2016; published 28 November 2016)

To investigate the systematics of mixed-symmetry states in $N = 52$ isotones, a relativistic Coulomb excitation experiment was performed during the PreSPEC campaign at the GSI Helmholtzzentrum für Schwerionenforschung to determine $E2$ transition strengths to 2^+ states of the radioactive nucleus ^{88}Kr. Absolute transition rates could be measured towards the first and third 2^+ states. For the latter a mixed-symmetry character is suggested on the basis of the indication for a strong $M1$ transition to the fully symmetric 2_1^+ state, extending the knowledge of the $N = 52$ isotones below $Z = 40$. A comparison with the proton-neutron interacting boson model and shell-model predictions is made and supports the assignment.

DOI: 10.1103/PhysRevC.94.054323

I. INTRODUCTION

The proton-neutron interacting boson model (IBM-2) [1] represents an algebraic formulation of a truncated shell model appropriate for the description of quadrupole collectivity. Because the IBM-2 is based on nucleon pairs formed by either two valence neutrons or two valence protons, it allows also the study of proton-neutron correlations, albeit of nucleon pairs approximated by bosons.

Dynamical symmetries, connected to the equations describing the dynamics of a quantal system, lead to conserved quantities denoted by quantum numbers and stringent selection rules which permit one to test the goodness of these quantum numbers. Furthermore, they give rise to a complete set of basis states, which can be constructed analytically. In the IBM-2 several dynamical symmetries can be constructed. Here we focus on those Hamiltonians that do not change upon exchange of the proton boson and neutron boson labels. Those can be classified using a new symmetry: F-spin symmetry [1]. A detailed account of the dynamical symmetries of these Hamiltonians is given in Ref. [2].

The concept of F spin in the IBM-2 extends the isospin formalism to the IBM-2 boson systems. These bosons are considered to be "elementary" particles that form a doublet with projection $F_z = +1/2$ (proton boson) and $F_z = -1/2$ (neutron boson). For the description of a given nucleus with fixed numbers of proton and neutron bosons, N_π and N_ν, respectively, the z component of the F spin is a good quantum number; it is $F_z = (N_\pi - N_\nu)/2$. For a given total boson number, $N = N_\pi + N_\nu$, the total F-spin quantum number can take values between F_z and $F_{\max} = N/2$.

While the low-lying collective states have $F = F_{\max}$ and are symmetric with respect to the pairwise exchange of boson F-spin labels, the IBM-2 predicts entire new classes of collective states with F-spin quantum numbers $F < F_{\max}$. Their wave functions contain at least one pair of proton and neutron bosons that is antisymmetric under the exchange of the proton and neutron labels. These states are called mixed-symmetry (MS) states.

In the mid-1980s the first MS state, a collective $J^\pi = 1^+$ excitation called scissors mode, was discovered in deformed gadolinium nuclei [3] by the research group of Richter. The IBM predicted the scissors mode [4] as one representative of the class of collective MS states in which valence neutron and proton pairs move out of phase. Scissors states were subsequently observed in many deformed nuclei and intensive theoretical studies of such states were performed [5,6].

According to the IBM-2 approach the whole class of MS states is formed by quadrupole collectivity. The building block of all MS excitations is therefore the MS 2^+_{ms} state. It should occur in spherical nuclei as the lowest, one-phonon MS state on which collective multiphonon structures can be built. The existence of such a multiphonon structure with MS character was discovered in the nuclide ^{94}Mo [7,8] and can be explained by the F-spin symmetric O(6) limit of the IBM-2 [2]. Recent measurements on ^{94}Mo and other $N = 52$ isotones confirm [9–15] the initial findings as a general phenomenon [16]. Here, the evolution of MS states in $N = 52$ isotones can be tracked over different proton shells. This enables the investigation of the variation of the proton-neutron interaction as a function of the nuclear valence space [17].

Unfortunately, the light $N = 52$ isotones below $Z = 40$ are unstable nuclei. No data on absolute transition rates of MS states existed prior to the present study. Absolute electromagnetic transition rates to low-lying states are, however, necessary information to uniquely identify MS states. Therefore, they are prerequisite for the systematic understanding of the proton-neutron nonsymmetric building blocks of nuclear collectivity.

It was the aim of this study to determine the quadrupole collectivity and to identify the lowest MS state of neutron-rich ^{88}Kr by using relativistic Coulomb excitation with a radioactive ion beam (RIB). Coulomb excitation is very well suited also for the population of one-phonon MS states [10,18,19]. The single-step Coulomb excitation reaction populates in a very clean way the excited 2^+ states. The desired $B(E2; 2^+_{ms} \to 0^+_1)$ and $B(M1; 2^+_{ms} \to 2^+_1)$ values can be deduced from the measured cross sections and branching ratios.

Recently, Mücher *et al.* were able to measure the $B(E2; 0^+_1 \to 2^+_1)$ in ^{88}Kr at REX-ISOLDE [14]. In that experiment it was also attempted to measure nonyrast states of ^{88}Kr, in particular the 2^+_3 state. However, using low-energy Coulomb excitation the cross section for the excitation of the MS state was more than three orders of magnitude smaller than the one for excitation of the 2^+_1 state. The result was that it was not possible to measure the $B(E2)$ of the 2^+_3 state. Using the predicted $B(E2; 0^+_1 \to 2^+_{ms})$ value, which is a factor of 10 weaker than the $B(E2; 0^+_1 \to 2^+_1)$ value [16], the cross section for Coulomb excitation using a ^{88}Kr beam at intermediate energy was calculated to be about two orders of magnitude higher than for the above-mentioned REX-ISOLDE measurement [20]. Thus, the PreSPEC setup at the GSI Helmholtzzentrum für Schwerionenforschung was chosen to obtain transition strengths for the possible MS candidate state in ^{88}Kr at 2216 keV. Figure 1 shows the relevant part of the level scheme of ^{88}Kr.

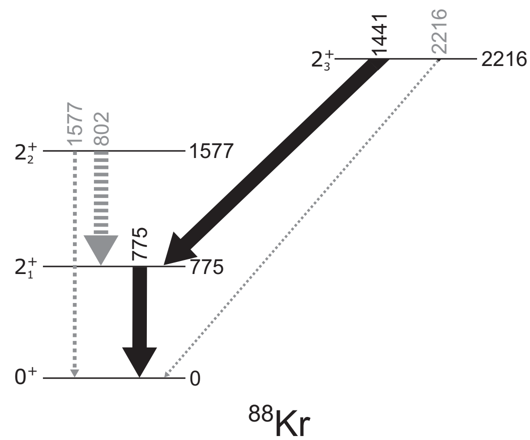

FIG. 1. Partial level scheme of ^{88}Kr illustrating the lowest lying 2^+ states and the known transitions between them. The thickness of the arrows expresses the branching ratios of the transitions adopted from Ref. [21]. Transitions that remained unobserved in this work are drawn with dashed grey lines. Energy labels are in keV.

II. EXPERIMENTAL DETAILS

A ^{238}U primary beam at 650 MeV/nucleon was provided by the GSI accelerator complex. The ^{88}Kr isotopes were produced by in-flight fission on a 0.66 g/cm^2 thick ^{9}Be primary target. The nuclei of interest were selected by the fragment separator (FRS) [22] utilizing the $B\rho$-ΔE-$B\rho$ method. For identification purposes the fission fragments were tracked by the FRS beam detectors in the middle and final focal plane on an event-by-event basis. By measurement of the time of flight (TOF) through the separator as well as the energy loss in a multiple sampling ionization chamber the composition of the secondary beam could be obtained. The FRS particle identification plot in terms of atomic number Z and mass-over-charge ratio A/Q is shown in Fig. 2. A clean separation of the isotope of interest was provided by full width at half maximum resolutions of 0.96% in A/Q and 0.91% in Z. A total of 2.0×10^6 ^{88}Kr nuclei could be identified during the experiment.

Coulomb excitation of the ^{88}Kr secondary beam at an energy of 128 MeV/nucleon took place on a 0.386 g/cm^2 thick, secondary ^{197}Au target. Deexcitation γ rays were detected by the PreSPEC Ge-detector array in the fast-beam configuration [23]. The array consisted of 15 EUROBALL Cluster detectors [24] placed under forward angles. The detection efficiency is enhanced due to the Lorentz boost of the γ-ray angular distribution at ion velocities of $\beta = v/c \sim 0.5$. The measurement was carried out using particle-γ coincidences to trigger the data acquisition. The ions after the secondary target were identified by the Lund-York-Cologne Calorimeter (LYCCA) [25], which acts as a $\Delta E - E$ telescope. Additionally, it provides the TOF and trajectory of the excited nuclei of interest after the target. This is particularly important to determine the velocity and scattering angles needed for a proper Doppler correction of the measured γ rays, as well as to ensure selection of safe Coulomb excitation events.

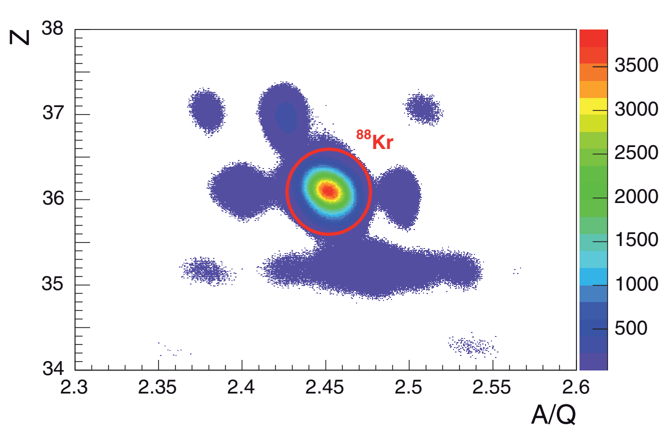

FIG. 2. FRS particle identification plot for the ^{88}Kr setting.

III. ANALYSIS

For the analysis of the Coulomb excitation, the same mass and charge numbers for ingoing and outgoing particles at the secondary target were selected. This was done by selecting events with proper A/Q and Z measured by the FRS particle detectors, as well as proper TOF, ΔE, and E determined by LYCCA. Further conditions on the scattering angle of ^{88}Kr and prompt time in the particle-γ coincidences were applied to select safe Coulomb excitation of the relativistic projectile and enhance the peak-to-background ratio of the obtained γ-ray spectra, respectively. By applying an event-by-event Doppler correction the $2_1^+ \rightarrow 0_1^+$ γ transition of ^{88}Kr at 775 keV could be clearly identified in the total γ-ray spectrum.

The EUROBALL Cluster detectors forming the PreSPEC array are arranged in two rings at mean polar angles of 16.3° and 34.7° comprising 5 and 10 cluster detectors, respectively. In the above-mentioned total γ-ray spectrum (both rings) for ^{88}Kr no clear evidence for Coulomb excitation of the 2_3^+ state could be observed. By separately considering detectors of the inner or outer rings, the spectra shown in Fig. 3 could be extracted.

While no clear peak structure in addition to the $2_1^+ \rightarrow 0_1^+$ transition is observed in the spectrum for the inner ring shown in Fig. 3(a), in the spectrum for the outer ring shown in Fig. 3(b) the region around 1441 keV exhibits significant excess of detected γ-ray events. This energy region corresponds exactly to the energy of the $2_3^+ \rightarrow 2_1^+$ transition in ^{88}Kr suggesting the Coulomb excitation of the 2_3^+ state. Other transitions in the spectrum are not observed. The rather broad and slightly asymmetric shape of the peak at 1441 keV is interpreted to originate from a very short lifetime of a few tens of femtoseconds, making it decay mainly while slowing down in the secondary target. Such fast transitions (short lifetimes) are expected for MS states due to high $B(M1; 2_{ms}^+ \rightarrow 2_1^+)$ values [16].

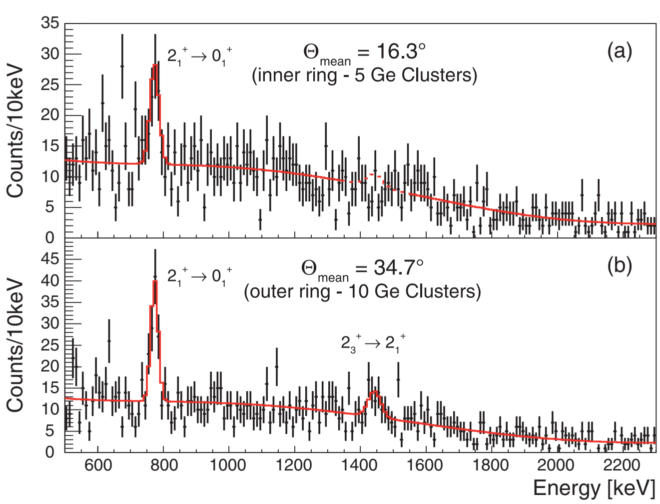

FIG. 3. Doppler-corrected γ-ray energy spectra for ^{88}Kr for the (a) inner and (b) outer ring of germanium detectors in the PreSPEC setup. The spectra are drawn with their statistical errors. Fits to the observed transitions and the 1σ observation limit in case of the $2_3^+ \rightarrow 2_1^+$ in the inner ring and a background function are indicated with the red (gray) line (see text for details).

The nonobservation in the inner ring can be understood considering the lower total efficiency due to fewer detectors in this group and the higher noise level due to more atomic background in close vicinity to the beam pipe.

Determining the peak areas in the spectrum for the outer ring for both transitions of ^{88}Kr led to values of 81(13) counts in the $2_1^+ \rightarrow 0_1^+$ and 29(10) counts in the $2_3^+ \rightarrow 2_1^+$ case. Considering the branching ratio of the $2_3^+ \rightarrow 2_1^+$ transition of 85.4(2)% [21] and an energy-dependent increase of detection efficiency of 35% for the lower lying line, we were able to extract the value for $B(E2; 0_{\rm g.s.}^+ \rightarrow 2_3^+)$ of ^{88}Kr by comparing the effective count rates. Normalizing to the value $B(E2; 0_{g.s.}^+ \rightarrow 2_1^+) = 0.093(9)\, e^2\mathrm{b}^2$ given in Ref. [14] we calculated a value of $B(E2; 0_{\rm g.s.}^+ \rightarrow 2_3^+) = 0.04(2)\, e^2\mathrm{b}^2$ or $B(E2\downarrow) = 3.4(17)$ W.u. Although small, this value exceeds the typical transition strength of a $2_{ms}^+ \rightarrow 0_1^+$ transition of about 1 W.u. A similar value of 3.7(8) W.u. was also observed for ^{92}Zr [12].

IV. RESULTS

The decay from the 2_3^+ state to the 2_1^+ state is most likely a nearly pure $M1$ transition. Figure 4 shows the experimentally obtained, normalized γ-ray intensities extracted for both rings with their 1σ error margins, including a 1σ upper limit for the 1441 keV transition due to the nonobservation in the inner ring [see Fig. 3(a)]. The experimental data was least-squares fitted with theoretical angular distribution functions calculated using the computer program DWEIKO [20]. The best description of the data (indicated by red lines in Fig. 4) results in a multipole mixing ratio $\delta = 0.08^{+0.09}_{-0.05}$ and indicates the preference for the $M1$ character for the $2_3^+ \rightarrow 2_1^+$ transition.

Assuming the determined $M1$ character a collective $B(M1; 2_3^+ \rightarrow 2_1^+)$ of 0.6(3) μ_N^2 is obtained in agreement with the expectations for a MS character of the 2_3^+ state. For the $E2$ transition strength we obtain a value of $B(E2; 2_3^+ \rightarrow 2_1^+) = 1.0^{+8.7}_{-0.9}$ W.u., which is in agreement within the error

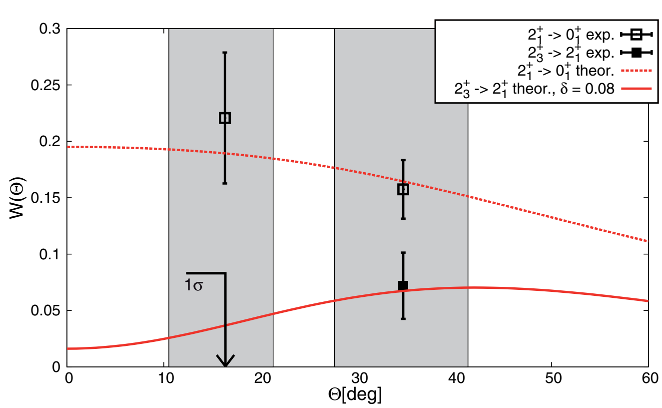

FIG. 4. Observed intensities with their statistical uncertainties (data points) and calculated angular distributions for the $2_1^+ \rightarrow 0_1^+$ with pure $E2$ character (dashed line) and the $2_3^+ \rightarrow 2_1^+$ (solid line) transitions. The angular range of the inner and outer rings of germanium detectors are marked with gray color. A 1σ observation limit is indicated for the $2_3^+ \rightarrow 2_1^+$ in the inner ring.

TABLE I. Deduced experimental transition strengths from the present data in comparison to model calculations in the IBM-2.

Transition	σL	$B(\sigma L)_{\text{expt}}$	$B(\sigma L)_{\text{O(6)}}$	$B(\sigma L)$ [26,27]
$2_2^+ \to 0_{\text{g.s.}}^+$	$E2$	$\leqslant$1.0 W.u.	forbidden	0.2 W.u.
$2_3^+ \to 0_{\text{g.s.}}^+$	$E2$	3.4(17) W.u.	0.8 W.u.	0.5 W.u.
$2_3^+ \to 2_1^+$	$E2$	$1.0^{+8.7}_{-0.9}$ W.u.	forbidden	0.6 W.u.
$2_3^+ \to 2_1^+$	$M1$	0.6(3) μ_N^2	0.30 μ_N^2	0.19 μ_N^2

bars both with the theoretical values (see Table I) and the value of $B(E2) = 5(3)$ W.u. obtained for the ^{94}Mo case [9].

In Fig. 3 there is no clear indication of an 802 keV line related to the $2_2^+ \to 2_1^+$ transition of ^{88}Kr. However, excitation of this state cannot be fully excluded due to the high statistical uncertainty of the γ-ray background. Estimating the sensitivity limit for clear identification of the γ-ray transitions to be ten counts, an upper limit of $B(E2; 0_{\text{g.s.}}^+ \to 2_2^+) \leqslant 0.012$ e^2b^2 for the excitation of this state follows. Table I lists the adopted values for the transition rates obtained from the present measurement and analysis.

V. DISCUSSION

Using the bare values for the boson g factors $g_n = 0$ and $g_p = 1.0\ \mu_N^2$ and effective quadrupole charges of $e_n = 0$ and $e_p = 0.07$ eb obtained in IBM-2 calculations of the even-even $^{88-96}$Kr isotopes [26,27], Table I gives the theoretical values in the F-spin symmetric O(6) limit [2] assuming ^{78}Ni as an inert core. Also given are the values obtained in Refs. [26,27] using IBM-2 parameters based on self-consistent mean-field calculations using a microscopic Gogny energy-density functional. In this calculation the 2_3^+ state is a mixed state with only 57% MS character. Better agreement of the experimental values is obtained for the O(6) limit which indicates a pure MS character for the 2_3^+ state.

Figure 5 shows the systematics for the even-even $N = 52$ isotones including our new data which fit the general behavior of the lowest MS states in this region. Although the dominant proton orbit changes from $g_{9/2}$ above ^{92}Zr to the upper part of the pf shell in ^{88}Kr, the collectivity of the lowest MS state remains at the same level. However, it should be noted that all experimentally known $B(M1; 2_{ms}^+ \to 2_1^+)$ in the $N = 52$ chain exceed the O(6) expectations.

For ^{94}Mo a good description of the $M1$ transition strength was obtained by a shell-model approach using the surface delta interaction (SDI) as the residual interaction and ^{88}Sr as an inert core [17]. Using the same model space, SDI parameters, and effective g factors a similar good agreement for the $B(M1; 2_{ms}^+ \to 2_1^+)$ value of one-phonon MS states in ^{92}Zr and ^{96}Ru is achieved. As pointed out in Ref. [12] these calculations show less good agreement with the experimentally obtained g factors for low-lying states in the $N = 52$ isotones.

To obtain a microscopic description below $Z = 40$, the shell-model valence space has to be enlarged with respect to the proton pf orbitals. Such an approach based on a ^{78}Ni core and an extended model space $(1f_{5/2}, 2p_{1/2}, 2p_{3/2}, 1g_{9/2})$ for protons and $(2d_{5/2}, 3s_{1/2}, 2d_{3/2}, 1g_{7/2}, 1h_{11/2})$ for neutrons was presented in Ref. [30] and reproduced spectroscopic data of mixed-symmetry states in zirconium isotopes as well as yrast excitations in ^{88}Kr [31]. With the same effective interaction but slightly changed effective charges of $e_n = 0.7$ eb, $e_p = 1.7$ eb, orbital g factors $g_l^n = 0$, $g_l^p = 1.0\ \mu_N^2$, and a quenching factor of 0.75 for the bare nucleon spin g factors, we obtained the theoretical energies and transition strengths for the 2_1^+ and 2_{ms}^+ states in ^{88}Kr, ^{90}Sr, and ^{92}Zr shown in Fig. 5. These shell-model calculations also predict mixed-symmetry states at the correct energies with clearly enhanced $B(M1; 2_{ms}^+ \to 2_1^+)$ values and $E2$ transitions to the ground state in good agreement with the experimentally observed strengths. However, the $B(M1)$ strengths are underestimated for ^{88}Kr and ^{92}Zr. Also, the wave-function analysis suggests that the identified states might not fully be the mixed-symmetric one-phonon 2_{ms}^+ states as pointed out for ^{92}Zr in Ref. [30]. The discrepancy between experiment and theory for the MS candidate state in ^{90}Sr at 1892 keV is larger and inverted (see Fig. 5). Here, the magnitude of the experimental transition strengths stems from a single lifetime measurement of $\tau = 3(2)$ ps using the $\beta\gamma\gamma$ fast timing method reported in Ref. [28]. A confirmation of this experimental lifetime is needed.

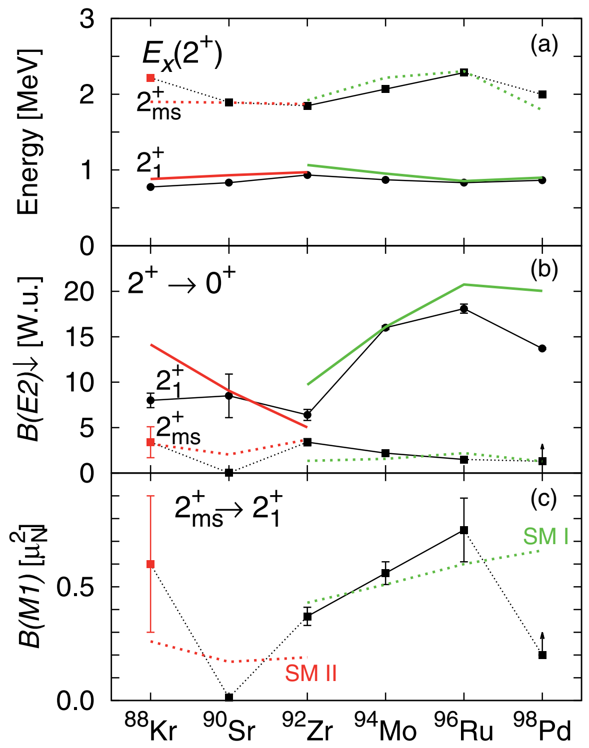

FIG. 5. (a) Excitation energies, (b) reduced $B(E2)$, and (c) $B(M1)$ transition strengths from the 2_1^+ and 2_{ms}^+ states in $N = 52$ isotones [13–16,28,29] together with the newly determined values for ^{88}Kr in red. Additionally shown are the results from shell-model calculations using the SDI [17] (green lines) and from new calculations based on the work of Ref. [30] (red lines).

VI. SUMMARY

In conclusion, we obtained $B(E2; 0^+_{\text{g.s.}} \rightarrow 2^+_3)$ and $B(M1; 2^+_3 \rightarrow 2^+_1)$ values as well as an upper limit for the $B(E2; 0^+_{\text{g.s.}} \rightarrow 2^+_2)$ value from relativistic Coulomb excitation of the radioactive nucleus ^{88}Kr. The strong $M1$ character of the $2^+_3 \rightarrow 2^+_1$ transition indicates the mixed-symmetric nature of the 2^+_3 state, which is supported by model calculations in the proton-neutron interacting boson model. New shell-model calculations for the $N = 52$ isotones ^{92}Zr, ^{90}Sr, and ^{88}Kr with a ^{78}Ni core also reproduce the measured transition strengths of the states in question.

ACKNOWLEDGMENTS

Parts of this research were carried out at the UNILAC/SIS accelerators at GSI Darmstadt, a member of the Helmholtz Association (HGF). This work was supported by the German BMBF under Contracts No. 06KY9136I, No. 05P12PKFNE, and No. 05P12RDFN8, HIC for FAIR, and the Swedish Research Council.

[1] A. Arima, T. Otsuka, F. Iachello, and I. Talmi, Phys. Lett. B **66**, 205 (1977).
[2] P. Van Isacker, K. Heyde, J. Jolie, and A. Sevrin, Ann. Phys. (NY) **171**, 253 (1986).
[3] D. Bohle, A. Richter, W. Steffen, A. E. L. Dieperink, N. Lo Iudice, F. Palumbo, and O. Scholten, Phys. Lett. B **137**, 27 (1984).
[4] F. Iachello, Nucl. Phys. A **358**, 89 (1981).
[5] A. Richter, Prog. Part. Nucl. Phys. **34**, 261 (1995).
[6] K. Heyde, P. von Neumann-Cosel, and A. Richter, Rev. Mod. Phys. **82**, 2365 (2010).
[7] N. Pietralla, C. Fransen, D. Belic, P. von Brentano, C. Frießner, U. Kneissl, A. Linnemann, A. Nord, H. H. Pitz, T. Otsuka, I. Schneider, V. Werner, and I. Wiedenhöver, Phys. Rev. Lett. **83**, 1303 (1999).
[8] N. Pietralla, C. Fransen, P. von Brentano, A. Dewald, A. Fitzler, C. Frießner, and J. Gableske, Phys. Rev. Lett. **84**, 3775 (2000).
[9] C. Fransen, N. Pietralla, Z. Ammar, D. Bandyopadhyay, N. Boukharouba, P. von Brentano, A. Dewald, J. Gableske, A. Gade, J. Jolie, U. Kneissl, S. R. Lesher, A. F. Lisetskiy, M. T. McEllistrem, M. Merrick, H. H. Pitz, N. Warr, V. Werner, and S. W. Yates, Phys. Rev. C **67**, 024307 (2003).
[10] N. Pietralla, C. J. Barton, R. Krucken, C. W. Beausang, M. A. Caprio, R. F. Casten, J. R. Cooper, A. A. Hecht, H. Newman, J. R. Novak, and N. V. Zamfir, Phys. Rev. C **64**, 031301 (2001).
[11] H. Klein, A. F. Lisetskiy, N. Pietralla, C. Fransen, A. Gade, and P. von Brentano, Phys. Rev. C **65**, 044315 (2002).
[12] V. Werner *et al.*, Phys. Lett. B **550**, 140 (2002).
[13] C. Fransen, A. Blazhev, A. Dewald, J. Jolie, D. Mücher, O. Möller, and T. Pissulla, AIP Conf. Proc. **1090**, 529 (2009).
[14] D. Mücher *et al.*, AIP Conf. Proc. **1090**, 587 (2009).
[15] A. Hennig, T. Ahn, V. Anagnostatou, A. Blazhev, N. Cooper, V. Derya, M. Elvers, J. Endres, P. Goddard, A. Heinz, R. O. Hughes, G. Ilie, M. N. Mineva, P. Petkov, S. G. Pickstone, N. Pietralla, D. Radeck, T. J. Ross, D. Savran, M. Spieker, V. Werner, and A. Zilges, Phys. Rev. C **92**, 064317 (2015).
[16] N. Pietralla, P. von Brentano, and A. F. Lisetskiy, Prog. Part. Nucl. Phys. **60**, 225 (2008).
[17] A. F. Lisetskiy, N. Pietralla, C. Fransen, R. Jolos, and P. von Brentano, Nucl. Phys. A **677**, 100 (2000).
[18] G. Rainovski, N. Pietralla, T. Ahn, C. J. Lister, R. V. F. Janssens, M. P. Carpenter, S. Zhu, and C. J. Barton, Phys. Rev. Lett. **96**, 122501 (2006).
[19] M. Danchev, G. Rainovski, N. Pietralla, A. Gargano, A. Covello, C. Baktash, J. R. Beene, C. R. Bingham, A. Galindo-Uribarri, K. A. Gladnishki, C. J. Gross, V. Y. Ponomarev, D. C. Radford, L. L. Riedinger, M. Scheck, A. E. Stuchbery, J. Wambach, C. H. Yu, and N. V. Zamfir, Phys. Rev. C **84**, 061306 (2011).
[20] C. Bertulani, C. Campbell, and T. Glasmacher, Comput. Phys. Commun. **152**, 317 (2003).
[21] E. McCutchan and A. Sonzogni, Nucl. Data Sheets **115**, 135 (2014).
[22] H. Geissel *et al.*, Nucl. Instrum. Methods Phys. Res. B **70**, 286 (1992).
[23] H. Wollersheim *et al.*, Nucl. Instrum. Methods Phys. Res. A **537**, 637 (2005).
[24] J. Eberth *et al.*, Prog. Part. Nucl. Phys. **28**, 495 (1992).
[25] P. Golubev *et al.*, Nucl. Instrum. Methods Phys. Res. A **723**, 55 (2013).
[26] M. Albers *et al.*, Phys. Rev. Lett. **108**, 062701 (2012); **109**, 209904 (2012); **114**, 189902 (2015).
[27] M. Albers *et al.*, Nucl. Phys. A **899**, 1 (2013); **947**, 260 (2016).
[28] H. Mach, F. Wohn, G. Molnár, K. Sistemich, J. C. Hill, M. Moszyński, R. Gill, W. Krips, and D. Brenner, Nucl. Phys. A **523**, 197 (1991).
[29] C. Fransen (unpublished).
[30] K. Sieja, F. Nowacki, K. Langanke, and G. Martínez-Pinedo, Phys. Rev. C **79**, 064310 (2009).
[31] M. Czerwiński, T. Rzaca-Urban, K. Sieja, H. Sliwinska, W. Urban, A. G. Smith, J. F. Smith, G. S. Simpson, I. Ahmad, J. P. Greene, and T. Materna, Phys. Rev. C **88**, 044314 (2013).